Biogeosciences Discuss., 8, 5179–5195, 2011
www.biogeosciences-discuss.net/8/5179/2011/
doi:10.5194/bgd-8-5179-2011

Biogeosciences Discussions

Coexisting methane and oxygen excesses in nitrate-limited polar water (Fram Strait) during ongoing sea ice melting

E. Damm, S. Thoms, G. Kattner, A. Beszczynska-Möller, E. M. Nöthig, and I. Stimac

Alfred Wegener Institute for Polar and Marine Research, P.O. Box 12061 27515 Bremerhaven, Germany

Received: 12 May 2011 – Accepted: 22 May 2011 – Published: 27 May 2011

Correspondence to: E. Damm (ellen.damm@awi.de)

Published by Copernicus Publications on behalf of the European Geosciences Union.

Abstract

Summer sea ice cover in the Arctic Ocean has undergone a reduction in the last decade exposing the sea surface to unforeseen environmental changes. Melting sea ice increases water stratification and induces nutrient limitation, which is also known to play a crucial role in methane formation in oxygenated surface water. We report on a hotspot of methane formation in the marginal ice zone in the western Fram Strait. Our study is based on measurements of oxygen, methane, DMSP, nitrate and phosphate concentrations as well as on phytoplankton composition and light transmission, conducted along the 79° N oceanographic transect. We show that between the eastern Fram Strait, where Atlantic water enters from the south and the western Fram Strait, where Polar water enters from the north, different nutrient limitation occurs and consequently different bloom conditions were established. Ongoing sea ice melting enhances the environmental differences and initiates regenerated production in the western Fram Strait. In a unique biogeochemical feedback process, methane production occurs despite an oxygen excess. We postulate that DMSP (dimethylsulfoniopropionate) released from sea ice may serve as a precursor for methane formation. Thus, feedback effects on cycling pathways of methane are likely, with DMSP catabolism in high latitudes possibly contributing to a warming effect on the earth's climate. This process could constitute an additional component in biogeochemical cycling in a seasonal ice-free Arctic Ocean. The metabolic activity (respiration) of unicellular organisms explains the presence of anaerobic conditions in the cellular environment. Therefore we present a theoretical model which explains the maintenance of anaerobic conditions for methane formation inside bacterial cells, despite enhanced oxygen concentrations in the environment.

1 Introduction

The Arctic Ocean is one of the regions in the world where climate change is most pronounced. Increased summer melting is considered to amplify biological production,

BGD
8, 5179–5195, 2011

due to the shift from an ice-covered to an open water Arctic Ocean (Arrigo et al., 2008). However, increasing water stratification during sea ice melting is likely to limit nutrient availability in near-surface water, which in turn hampers the enhancement of primary production (Sakshaug, 2003). A characteristic feature of the Arctic Ocean is the distinct post-bloom nutrient limitation found in the Atlantic-dominated and Pacific-dominated sectors. The former is nitrate and phosphate co-limited while the latter is mostly nitrate-limited, which results in an excess of phosphate (Yamamoto-Kawai et al., 2006). These different nutrient limitations can stimulate the growth of specific members of the bacterioplankton assemblage with consequences not only for the turnover of organic matter, biogeochemical cycling of carbon but also for producing climate relevant trace gases (Thingstad et al., 2008). In this context the degradation of DMSP (dimethylsulfoniopropionate) becomes pivotal. DMSP is produced by marine phytoplankton and when metabolized, a primary carbon source for heterotrophic bacteria (Kiene et al., 2000). DMSP is the precursor of DMS (dimethylsulfide) or methanethiol. DMS partly escapes to the atmosphere where it is the most important climate-cooling gas, counterbalancing the effect of greenhouse gases (Charlson et al., 1987). Methanethiol is a key reactive intermediate utilized as sulfur and carbon sources for biosynthesis or energy generation (Kiene et al., 2000). In anaerobic environments methanethiol is also a precursor of methane production (Tallant and Kryzcki, 1997). A switch in the utilization of phosphate and DMSP degradation products in nitrate-limited Pacific-derived water is also considered to produce methane in aerobic environments (Damm et al., 2010). While the role of nutrient limitation as a possible regulator of methane production has only recently been investigated (Karl et al., 2008), methane excess in ocean surface water relative to the atmospheric equilibrium has been studied for more than three decades (Scranton and Brewer, 1977). Very recently, methane excess in surface water has also been detected under multi-year sea ice and in the marginal ice zone along the North-West Passage, i.e. the region from the southwest edge of Greenland through the Baffin Bay to the Beaufort Sea (Kitidis et al., 2010).

BGD
8, 5179–5195, 2011

Here we present data from Fram Strait where Atlantic water and Pacific-derived surface water bodies occur adjacent to each other. We show that ongoing sea ice melting has amplified the environmental differences between both water masses and that methane production occurred during regenerated production in Pacific-derived water despite an apparent oxygen excess. Because methanogenesis as an anaerobic process is not expected to occur in aerobic environments we determine the maximum oxygen concentration in seawater, which allows anaerobic processes to take place inside bacterial cells. Since this aspect is fundamentally important we provide a detailed model description to show and explain why and how it can potentially occur.

2 Regional setting

In the Fram Strait, the surface water (<60 m) in general comprises two main water masses, which flow in opposite directions (Rudels et al., 2000). The warm (up to 4 °C) and saline (up to 34.8) Atlantic water (AW) branch flows northward east of about 4° W (Fig. 1). Further west, colder and less saline polar surface water (PSW) occupies the upper water column. In PSW, a portion is Pacific-derived water that varies inter-annually between more than 90 % (Jones et al., 2003) to almost zero (Falck et al., 2005). In 2008, this portion had attained just over 60 % (Dodd et al., 2011). Salinity of PSW was homogeneous at about 33 indicating unchanged conditions since winter convection, except for some near-surface warming and freshening by melt water (Fig. 2a). This distribution has been described previously for the end of the summer season (Budeus et al., 1997).

The recurrent Northeast Water Polynya (NEWP) is localized in the region of the PSW (Budeus and Schneider, 1995). Polynyas are less light-limited due to early opening of the ice cover compared to adjacent regions, and primary production starts earlier in the year. In the NEWP, the shift from eutrophic to oligotrophic conditions is reported to occur at the end of July (Wallace et al., 1995, Kattner and Budeus, 1997). In the summer of 2008, ice fields drifting from the north partly covered the transect region

BGD
8, 5179–5195, 2011

(Fig. 1). Hence stations in the middle of transect were located in partly ice-covered AW and PSW and the more eastern and western stations in ice-free AW and PSW, respectively.

3 Sampling procedure

In summer 2008, a hydrographic transect was carried out with the RV "Polarstern" in the Fram Strait, roughly along 79° N (Fig. 1). Salinity, temperature, light transmission and oxygen were measured with a Seabird SBE 911+ CTD and C-Star Wetlabs transmissiometer. Water samples for estimating phytoplankton abundances of dominant unicellular organisms were collected with a Niskin rosette sampling system and with an Apstein net 20 µm mesh size towed through the upper 10 m water column. Phyto- and protozooplankton samples obtained were preserved in hexamine-buffered formalin (final concentration of ~1 %). In aliquots cells of the dominant species or groups were counted with an inverted microscope. Nutrient analyses were performed on board with a nutrient analyzer (Evolution III, Alliance Instruments) according to standard methods. Methane concentration was analyzed within hours of sampling. The dissolved gas was extracted from water by vacuum-ultrasonic treatment and subsequently measured with a gas chromatograph (Chrompack 9003 (GC) with a flame ionization detector (FID). For gas chromatographic separation we used a packed column (Porapac Q 80/100 mesh). The GC oven was operated isothermally (60 °C) and the heated zone of the FID was held at a temperature of 250 °C. Two sets of standard gas mixtures were used for calibration. The standard deviation of duplicate analyses was 5 %. This high overall error is almost exclusively due to the gas extraction procedure and not to GC precision, which had an error of only 1 %.

Total DMSP samples were collected directly from Niskin sample bottles into 50 ml centrifuge tubes that contained 167 µl of 50 % H_2SO_4. The tubes were sealed and the samples stored for later analysis on shore. DMSP is stable for months in acidic solution (Curran et al., 1999). Dissolved DMSP samples were collected by the small volume

BGD
8, 5179–5195, 2011

drip filtration procedure recommended by Kiene and Slezak (2006). Briefly, about 50 ml of seawater was allowed to flow into a 47 mm filter tower that held a Whatman GF/F glass fiber filter. The water was allowed to drip through the filter and only the first 3.5 ml of filtrate was collected directly into a storage tube that contained 50 µl of 50 % H_2SO_4. DMSP in the stored samples was analyzed as DMS after alkaline cleavage. A subsample of the solution was pipetted into a 14 ml serum vial and treated with 1 ml of 5 N NaOH and quickly sealed. The released DMS was purged into a cryotrap and quantified with a gas chromatograph equipped with a Chromosil 330 column and a pulsed flame photometric detector (PFPD). Helium was used as the purge gas and the carrier gas.

4 Results and discussion

4.1 Nutrient limitation and biological production

In AW with ice cover, nitrate and phosphate were abundant but depleted in open water while the Redfield ratio remained preserved as well as in ice-covered and ice-free AW. In both ice-covered and ice-free PSW, nitrate was undetectable in near-surface water (<20 m) and became limiting before phosphate (Fig. 2b and c). Hence, PSW was characterized by lower nitrate to phosphate ratios than the normal Redfield ratio as also reported by Yamamoto-Kawai et al. (2006).

In accordance with the varying nitrate availability and ice cover, different bloom stages were prevalent, also indicated by the varying light transmission. In ice-free AW, light transmission was reduced down to a depth of 60 m. This feature is in accordance with a typical late bloom population which was observed in the non-stratified water column east of 1° E (Fig. 2b and d). Next to the dominating prymnesiophyte *Phaeocystis pouchetii*, many heterotrophic unicellular specimens were found belonging to dinoflagellates and ciliates. Diatoms comprised a few *Thalassiosira* spp and very few pennates. The occurrence of the two coccolithophores *Emiliania huxleyi* and

BGD
8, 5179–5195, 2011

Coccolithus pelagicus was indicative of minor ice influence. An impoverished phytoplankton community and a high light transmission were found in the nitrate-limited ice-free PSW (Fig. 2d, west of 10° W).

In the ice-covered regions light transmission was reduced up to a depth of 20 m. However, the varying nitrate availability created different under ice bloom situations: the AW was dominated by large *Phaeocystis pouchetii* colonies, which were partly covered with tiny pennate diatoms, whereas in the PSW cold water ice-related algal communities were observed.

4.2 Melting sea ice in nitrate-limited environment – biogeochemical consequences

The environmental differences between both water masses obviously influence the under ice bloom conditions. New production occurred in the largely ice-covered AW. The almost constant nitrate/phosphate ratios, which correlated with increasing oxygen concentrations, substantiate this observation (Fig. 2e and h). By comparison, a shift from new to regenerated production is obviously evident in nitrate-limited PSW, reflected in the increasing perturbation of the Redfield ratio coupled with a pronounced oxygen enhancement (Fig. 2e and h). This shows that sources of nitrogen other than nitrate may be important in supporting the productivity. In the Fram Strait region, ammonium is released from multi-year Arctic sea ice potentially alleviating the nutrient limitation (Tovar-Sanchez et al., 2010). This would mean that in PSW, where an excess of phosphate is available, ammonium could be an alternative nitrogen source for regenerated production.

In addition, during regenerated production the ability of bacteria to compete with the phytoplankton community for inorganic nutrients and organic material is enhanced (Thingstad et al., 2008). Hence, melting sea ice in PSW may also affect the microbial food web. An important energy, carbon and sulfur source for bacterial biomass production is DMSP (Kiene et al., 2000). Actually, both water masses also differed clearly with regard to their DMSP concentrations (Fig. 2f). The high concentrations in ice-free AW

BGD
8, 5179–5195, 2011

were probably due to DMSP release by senescing *Phaeocystis pouchetii* cells, which are known to be major producer of DMSP in polar waters (Matrai and Vernet, 1997). The low DMSP concentrations in ice-free PSW may be the result of an impoverished bloom of almost non DMSP producing diatoms, but also due to an enhanced bacterial utilization of DMSP.

In contrast, enhanced DMSP concentrations are to be expected in ice-covered water masses because substantial amounts of DMSP are produced by ice algae released from melting sea ice (Levasseur et al., 1994; Uzuka, 2003). DMSP concentrations comparable to those in ice-free AW were detected in ice-covered AW, despite the early bloom stage, which confirms additional DMSP release by sea ice. However, in ice-covered PSW, DMSP concentrations were comparably low as in ice-free PSW, despite a potential input of ice-released DMSP. This would imply that in ice-covered PSW, where regenerated production occurred, DMSP was depleted due to enhanced bacterial consumption. Consequently the fate of DMSP released by melting ice would be related to the nutrient status in the water column.

Comparable to DMSP, methane concentrations also differed clearly between the two water masses. In AW, methane tended to be equilibrated or slightly under-saturated in relation to the atmospheric concentration, which is estimated to be between 3 and 3.5 nM, depending on temperature and salinity. A slight oversaturation was found in ice-free PSW, which may be generated by methane release from the seafloor in the NEWP region, which is localized on the shelf with up to only 100 m water depths. In shallow Polynya regions enhanced turbulence during convective mixing enhances sediment resuspension and eventually methane release from the seafloor (Damm et al., 2007). However, in comparison the methane excess in ice-covered PSW clearly rises above the slight oversaturation detected in ice-free PSW.

It is striking that this methane surplus is localized in the region where regenerated production occurred and where DMSP was clearly depleted (Fig. 2). This pattern is similar to that in the central Arctic Ocean where a change in the utilization of phosphate and methylated compounds is found to trigger the switch from no methane production

BGD
8, 5179–5195, 2011

to methane production in Atlantic and Pacific surface water, i.e. in nitrate/phosphate co-limited and nitrate-limited water (Damm et al., 2010). In addition, the methane excess detected under multi-year-sea-ice and in the marginal ice zone along the North-West Passage (Kiditis et al., 2010) also occurs in a region, which receives Pacific-derived water after its journey through the Arctic Ocean (Jones et al., 2003).

We therefore conclude that the development of a hotspot of methane production is a rapid response during regenerated production when melting sea ice supplies DMSP as an additional carbon source. In comparison: in ice-covered AW, replete with nitrate and phosphate, new production occurred and DMSP was clearly enriched, no methane excess was observed. An inverse correlation of DMSP with methane suggests that DMSP may serve as precursor for methane production as found in surface polar shelf water in Storfjorden (Spitsbergen). This is additionally confirmed by the in situ-produced methane, depleted in ^{13}C, which is directly related to the decreasing DMSP/methane relationship, corroborating the interaction between both parameters (Damm et al., 2008).

Further, the microbial degradation of DMSP to methane was observed in a microcosm experiment carried out with seawater from the Fram Strait during that cruise (Damm et al., 2010). During the experiment *Archaea abundance* remained negligible and bacteria of the *Rhodobacter/Roseobacter* were dominant. A survey of available *Roseobacter* genomes by Moran et al. (2007) revealed that 50 % of the genomes contained genes for DMSP demethylation.

5 Contemporary methane and oxygen excess – a paradox?

It is conspicuous that oxygen concentrations in surface waters did not hamper methane production (Fig. 2e and g). As methanogenic activity is not favored in aerobic environment it was assumed that this process occurs in microenvironments which are sufficiently lacking in molecular oxygen (Cynar and Yayanos, 1992). The limiting conditions for the maintenance of a reduced micro-niche within oxidized marine sediments were

BGD
8, 5179–5195, 2011

first discussed by Jørgensen (1977). The question arises whether reducing conditions can exist within a *Roseobacter* cell, which would allow anaerobic processes inside the bacterial cell. To answer this question, we extended the model of Jørgensen (1977) by an additional compartment for the cell membrane and calculated the oxygen concentration profile in the interior of the cell as a function of the cell properties (cell size, rates of respiratory metabolism, membrane permeability for O_2) and the external O_2 concentration.

We describe the bacterial cell in terms of a sphere of radius b covered by a thin membrane. The membrane is described by a homogeneous spherical shell of outer and inner radii a and b. Within the interior of the sphere there is an O_2 consumption of constant intensity ρ. To determine the stationary concentration profile in the interior of the sphere we have to find the solution in the region $0 \le r \le b$ of

$$D\frac{1}{r^2}\frac{d}{dr}\left(r^2\frac{dC(r)}{dr}\right)-\rho(r)=0, \tag{1}$$

where D is the diffusivity of O_2 and $C(r)$ is the concentration of O_2 as a function of the radial distance r from the centre of the cell. Integrating and solving the equation for $\rho(r)=\rho$ and finite concentrations at $r=0$ yields

$$C(r)=C_b-\frac{\rho}{6D_w}\left(b^2-r^2\right), \tag{2}$$

where $C_b = C(r=b)$ is the concentration in the sphere at the inner side of the membrane and D_w is the diffusion coefficient in water. To determine C_b we consider stationary diffusion through the membrane of thickness $h = a - b$ and with a permeability P for O_2. It is assumed that there is no O_2 consumption in the membrane region. Hence in the region $b \le r \le a$, Eq. (1) is integrated for $\rho(r)=0$. With the total flux of O_2 through the membrane F (units: mol $O_2\,s^{-1}$), integration of Eq. (1) gives the following expression for C_b as a function of the concentration at the cell surface, $C_a = C(r=a)$,

$$C_b=C_a-\frac{F}{4\pi D_m}\frac{a-b}{ab}, \tag{3}$$

BGD
8, 5179–5195, 2011

where D_m is the diffusion coefficient in the membrane and F equals the total O_2 consumption in the region $0 \le r \le b$, which is given by the respiration rate per cell, i.e. $F = {}^4/_3 \pi b^3 \rho$. We consider the situation where the thickness of the membrane $h = a - b$ is small in proportion to the radius b. In that case $ab \approx b^2$, and Eq. (3) takes the form

$$C_b = C_a - \frac{F}{4\pi b^2}\frac{h}{D_m} = C_a - \frac{F}{4\pi b^2}\frac{1}{P} = C_a - \frac{\rho}{3}\frac{b}{P}. \quad (4)$$

To determine C_a we have to find the stationary concentration profile in the cell environment by solving Eq. (1) for $\rho(r) = 0$ in the region $r \ge a$. With $C(r \to \infty) = C_0$, integration of Eq. (1) yields

$$C(r) = C_0 - \frac{F}{4\pi D_w}\frac{1}{r} = C_0 - \frac{\rho}{3D_w}\frac{b^3}{r}, \quad (5)$$

where C_a follows for $r = a \approx b$. Replacing this value for C_a in Eq. (4) and the result for C_b in Eq. (2) gives

$$C(r) = C_0 - \frac{\rho b^2}{3D_w} - \frac{\rho b}{3P} - \frac{\rho}{6D_w}\left(b^2 - r^2\right), \quad (6)$$

which is the equation for the concentration profile in the interior of the cell. The profile is a parabola with the minimum of O_2 concentration at $r = 0$. When $C(r)$ is zero for $r = 0$ we obtain the following equation for the maximum concentration in the environment, $C_{0,\max}$, which allows anaerobic processes to take place inside the cell:

$$C_{0,\max} = \frac{\rho b^2}{2D_w} + \frac{\rho b}{3P}. \quad (7)$$

For a salinity of 33 at 0 °C, the diffusion coefficient of O_2 in water is $D_w = 1.05 \times 10^{-9}\,\mathrm{m^2\,s^{-1}}$ (Ramsing and Gundersen, 1994). The respiration per cell, 0.61 fmol $O_2\,\mathrm{h^{-1}}$, was measured in laboratory experiments with *Roseobacter* cultures

BGD
8, 5179–5195, 2011

grown in a chemostat at 22 °C (Koblížek et al., 2010). The simplest correction for temperature of bacterial respiration is the temperature coefficient, Q_{10}, the factor by which a biological reaction changes with a temperature increase of 10 °C. The model of Rivkin and Legendre (2001) predicts a Q_{10} of 1.85 for bacterial respiration (Vázquez-Domínguez et al., 2007). The respiration rate measured at 22°C is thus reduced by a factor of $1/Q_{10}^{2.2} = 0.26$ for an environmental temperature of ~0 °C. In the following a respiration rate per cell of $F = 0.16\,\mathrm{fmol\,O_2\,h^{-1}}$ at 0 °C is therefore assumed. Using the cell volume of $0.53\,\mu\mathrm{m}^3$ obtained in the laboratory experiments with *Roseobacter* (Koblížek et al., 2010), it follows the radius of the sphere, $b = 0.5\,\mu\mathrm{m}$, and the constant intensity of O_2 consumption in the interior of the sphere, $\rho = 0.084\,\mathrm{mol\,m^{-3}\,s^{-1}}$. Permeabilities for gases of bacteria and microalgae have been determined in very few investigations. The membrane permeability for O_2 (P) follows from the permeability for CO_2 (P_{CO_2}) by the relationship (Spalding and Portis, 1985)

$$P = P_{CO_2}\sqrt{\frac{\text{molecular weight of } CO_2}{\text{molecular weight of } O_2}}. \tag{8}$$

Using $P_{CO_2} = 3\times10^{-8}\,\mathrm{m\,s^{-1}}$, as measured for *Synechococcus* UTEX 625 (Salon et al., 1996), one obtains $P = 3.5\times10^{-8}\,\mathrm{m\,s^{-1}}$. From Eq. (7) it now follows that the maximum O_2 concentration in the environment which allows anaerobic processes to take place inside the bacterial cell, is $C_{0,\max} = 400\,\mu\mathrm{M}$. The latter corresponds to the O_2 concentrations observed in nitrate-limited PSW in the region where the highest methane concentrations were observed (Fig. 2e and g). Hence, in this PSW we had the situation where oxygen decreased almost to zero in the interior of the bacterial cell, but was present in the membrane region and outside the cell. The above calculations demonstrate that an oxygen excess in the surrounding medium does not exclude the establishment of anaerobic conditions within the bacterial cell. Altogether our model results suggest that oxygen excess and methane production are not mutually exclusive.

BGD
8, 5179–5195, 2011

Acknowledgements. We thank the scientific party and crew of RV Polarstern for their support at sea.

References

Arrigo, K. A., van Dijken, G. and Pabi, S.: Impact of a shrinking Arctic ice cover on marine primary production, Geophys. Res. Lett., 35, L19603, doi:10.1029/2008GL035028, 2008.

Budeus, G. and Schneider, W.: On the hydrography of the Northeast Water Polynya, J. Geophys. Res., 100, 4287–4299, 1995.

Budeus, G., Schneider, W., and Kattner, G.: Distribution and exchange of water masses in the Northeast water Polynya (Greenland Sea), J. Mar. Syst., 10, 123–138, 1997.

Charlson, R. J., Lovelock, J. E., Andreae, M. O., and Warren, S. G.: Oceanic phytoplankton, atmospheric sulfur, cloud albedo and climate, Nature, 326, 655–661, 1987.

Curran, M. A. J., Jones, G. B., and Burton, H.: Spatial distribution of dimehylsulfide and dimethylsulfoniopropionate in the Australian sector of the southern ocean, J. Geophys. Res., 103, 16667–16689, 1999.

Cynar, F. J. and Yayanos, A. A.: The distribution of methane in the upper waters of the southern California Bight, J. Geophys. Res., 97(C7), 11269–11285, 1992.

Damm, E., Schauer, U., Rudels, B., and Hass, C.: Excess of bottom-released methane in an Arctic shelf sea polynya in winter, Cont. Shelf Res., 27(12), 1692–1701, 2007.

Damm, E., Kiene, R. P., Schwarz, J. Falck, E., and Dieckmann, G.: Methane cycling in Arctic shelf water and its relationship with phytoplankton biomass and DMSP, Mar. Chem., 109, 45–59, 2008.

Damm, E., Helmke, E., Thoms, S., Schauer, U., Nöthig, E., Bakker, K., and Kiene, R.: Methane production in aerobic oligotrophic surface water in the central Arctic Ocean, Biogeoscience, 7, 1099–1108, 2010.

Dodd, P. A., Rabe, B., Hansen, E., Mackensen, A., Rohling, E., Falck, E., Reigstad, M., Jones, P., Schauer, U., and Stedmon, C.: The Freshwater Composition of the Fram Strait Outflow Derived from a Decade of Tracer Measurements, in preparation, 2011.

Falck, E., Kattner, G., and Budeus, G.: Disappearance of Pacific Water in the northwestern Fram Strait, Geophys. Res. Lett., 32, L14619, doi:10.1029/2005GL023400, 2005.

Jones, E. P., Swift, J. H., Anderson, L. G., Lipizer, M., Civitarese, G., Falkner, K. K., Kattner, G.,

BGD

8, 5179–5195, 2011

and McLaughlin, F. A.: Tracing Pacific Water in the North Atlantic Ocean, J. Geophys. Res., 108(C4), 3116, doi:10.1029/2001JC001141, 2003.
Jørgensen, B. B.: Bacterial sulphate reduction within reduced microniches of oxidized marine sediments, Mar. Biol., 41, 7–17, 1977.
Karl, D. M., Beversdorf, L., Björkman, K., Church, M. J., Martinez, A., and DeLong, E. F.: Aerobic production of methane in the sea, Naturegeoscience, 1, 473–478, doi:10.1038/ngeo234, 2008.
Kattner, G. and Budeus, G.: Nutrient status of the Northeast Water Polynya, J. Mar. Syst., 10, 185–197, 1997.
Kiene, R. P., Linn, L. J., and Bruton, J. A.: New and important roles for DMSP in marine microbial communities, J. Sea Res., 43, 209–224, 2000.
Kitidis, V., Upstill-Goddard, R. C., and Anderson, L. G.: Methane and nitrous oxide in surface water along the North-West Passage, Mari. Chem., 121, 80–86, 2010.
Koblížek, M., Mlèoušková, J., Kolber, Z., and Kopecký, J.: On the photosynthetic properties of marine bacterium COL2P belonging to *Roseobacter* clade, Arch Microbiology, 192, 41–49, 2010.
Levasseur, M., Gosselin, M., and Michaud, S.: A new source of dimethylsulfide (DMS) for the Arctic atmosphere: ice diatoms, Mar. Biology, 121, 181–187, 1994.
Matrai, P. A. and Vernet, M.: Dynamics of the vernal bloom in the marginal ice zone of the Barents Sea: Dimethylsulfide and Dimethylsulfoniopropionate budgets, J. Geophys. Res., 102, C10, 22965–22979, 1997.
Moran, M. A., Belas, R., Schell, M. A., Gonzalez, J. M., Sun, F., Sun, S., Binder, B. J., Edmonds, B., Ye, J. W., Orcutt, B., Howard, E. C., Meile, C., Palefsky, W., Goesmann, A., Ren, Q., Paulsen, I., Ulrich, L. E., Thompson, L. S., Saunders, E., and Buchan, A.: Ecological genomics of marine Roseobacters, Appl. Environ. Microbiol. 73, 4559–4569, 2007.
Ramsing, N. and Gundersen, J.: Tabulated physical parameters of interest to people working with microsensors in marine systems, Techn. Rep. MPI Mar. Microbiology, Bremen, 1994.
Rivkin, R. B. and Legendre, L.: Biogenic carbon cycling in the upper ocean: Effects of microbial respiration, Science, 291, 2398–2400, 2001.
Rudels, B., Meyer, R., Fahrbach, E., Ivanov, V., Osterhus, S., Quadfasel, D., Schauer, U., Tverberg, V., and Woodgate, R.: Water mass distribution in Fram Strait and over the Yermak Plateau in summer 1997, Ann. Geophys., 18, 687–705, 2000.
Sakshaug, E.: Primary and secondary production in the Arctic Seas, in *The Organic Carbon*

BGD
8, 5179–5195, 2011

Cycle in the Arctic Ocean, edited by: Stein, R. and McDonald, R. W., 57–81, Springer, Berlin, 2003.
Salon, C., Mir, N. A., and Canvin, D. T.: Influx and efflux of inorganic carbon in *Synechococcus* UTEX 625, Plant. Cell. Environ., 19, 247–259, 1996.
Scranton, M. I. and Brewer, P. G.: Occurrence of methane in the near surface waters of the western subtropical North-Atlantic, Deep-Sea Res., 24, 127–138, 1977.
Spalding, M. H. and Portis, A. R.: A model of carbon dioxide assimilation in *Chlamydomonas reinhardtii*, Palta, 164, 308–320, 1985.
Spreen, G., Kaleschke, L., and Heygster, G.: Sea ice remote sensing using AMSR-E 89 GHz channels, J. Geophys. Res., 113, C02S03, doi:10.1029/2005JC003384, 2008.
Tallant, T. C. and Krycki, J. A.: Methylthiol: coenzyme M methyltransferase from methanosarcina barkeri, an enzyme of methangenesis from dimethylsulfide and methylmercatopropionate, J. Bacteriol., 179, 6902–6911, 1997.
Thingstad, T. F., Bellerby, R. G. J., Bratbak, G., Borsheim, K. Y. Egge, J. K., Heldal, M., Larsen, A., Neill, C., Nejstgaard, J., Norland, S., Sandaa, R. A., Skoldal, E. F., Tanaka, T., Thyraug, R., and Töpper, B.: Counterintuitive carbon-to-nutrient coupling in an Arctic pelagic ecosystem, Nature, 455,387–390, doi:10.1038/nature07235, 2008.
Tovar-Sanchez, A., Duarte, C. M., Alonso, J. C., Lacorte, S., Tauler, R., and Galban-Malagon, C.: Impacts of metals and nutrients released from melting multiyear Arctic sea ice, J. Geophys. Res., 115, C07003, doi:10.1029/2009JC005685, 2010.
Uzuka, N.: A time series observation of DMSP production in the fast ice zone near Barrow (extended abstract), Tohoku Geophys. Journ. (Sci. Rep. Tohoku Univ., Ser. 5), 36(4), 439–442, 2003.
Vázquez-Domínguez, E., Vaqué, D., and Gasol, J. M.: Ocean warming enhances respiration and carbon demand of coastal microbial plankton, Glob. Change Biol., 13, 1327–1334, doi:10.1111/j.1365-2486.2007.01377.x, 2007.
Wallace D. W. R., Minnett, P. J. and Hopkins, T. S.: Nutrients, oxygen and inferred new production in the Northeast Water Polynya, J. Geophys. Res., 100(C3), 4323–4340, 1995.
Yamamoto-Kawai, M., Carmack, E. C., and McLaughlin, F. A.: Nitrogen balance and Arctic throughflow, Nature, 443, p. 43, 2006.

BGD
8, 5179–5195, 2011

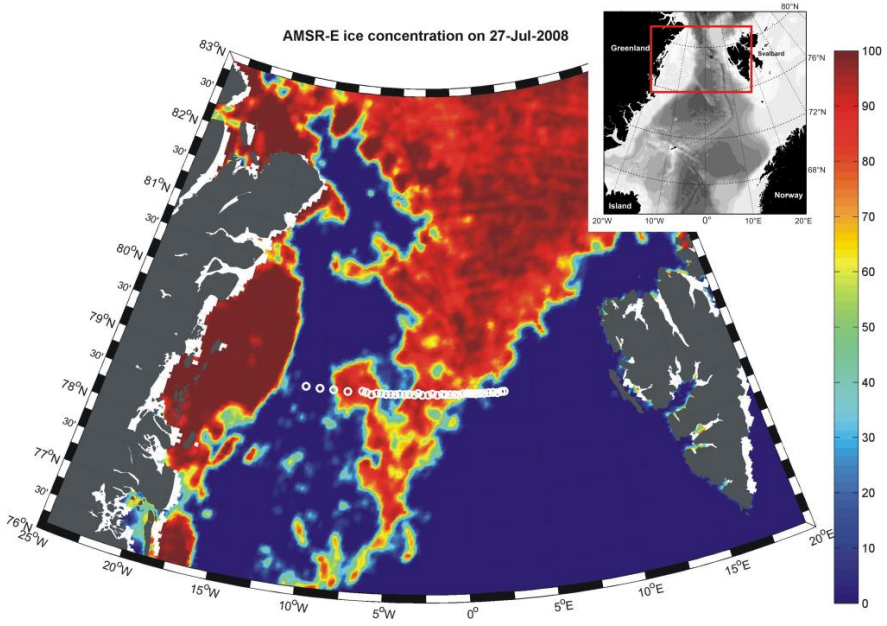

Fig. 1. Map of the Fram Strait (AMSR-E data see Spreen et al, 2008), white circles are stations.

BGD
8, 5179–5195, 2011

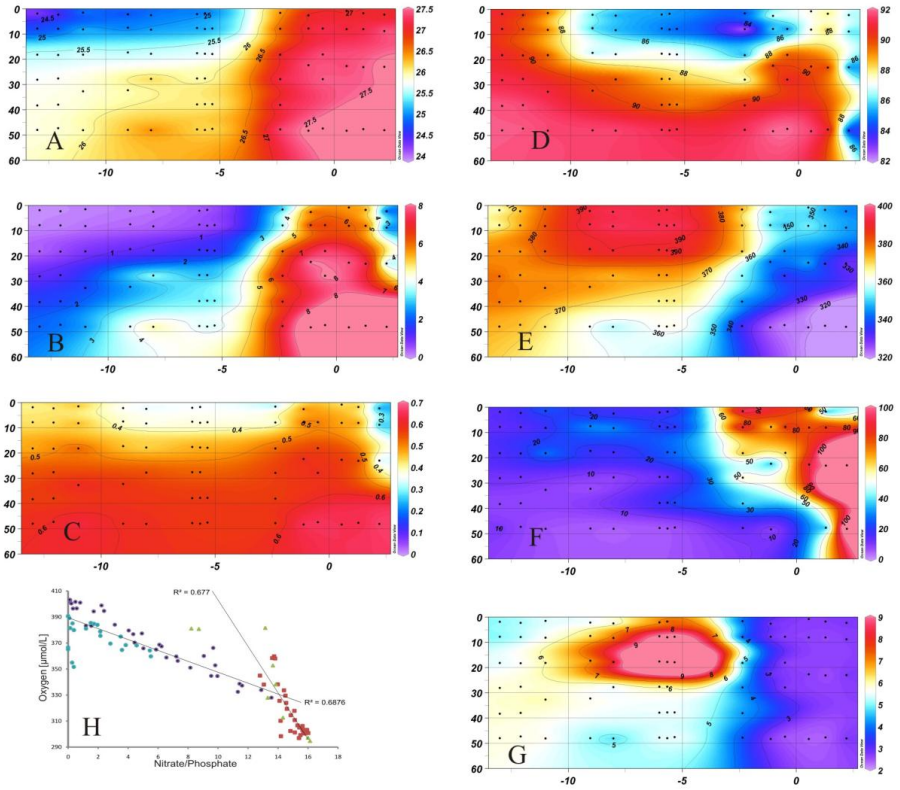

Fig. 2. Profiles (black dots) along the transect from 15° W to 4° E; diagrams show: potential density in sigma θ units **(A)**, concentrations of nitrate, phosphate and oxygen (µmol/l) **(B, C, E)**, light transmission (%), **(D)**, concentrations of DMSP and methane (nM), **(F)** and **(G)**. H shows the nitrate/phosphate ratios vs. oxygen; black/green dots are ice-covered and ice-free Polar Surface water (PSW), respectively, red squares/green triangles are ice-free and ice-covered Atlantic water (AW).

BGD
8, 5179–5195, 2011